Fabrication of a nanophotonic quantum dot waveguide and photodetector integrated device

L. Huang, M.C. Hegg, C.-J. Wang and L.Y. Lin

Abstract: The authors present the design and fabrication of a nanophotonic waveguide and photodetector integrated device by molecular self-assembly of nanocrystal quantum dots (QD) and two different nano-gap formation techniques, namely electromigration-induced break-junction technique and electron beam lithography nano-gap patterning. A QD waveguide with ∼50 nm width integrated with a nano-scale QD photodetector is achieved. A comparison is made between the two nano-gap techniques. In addition, a method to achieve high alignment accuracy for nanophotonic integration is discussed.

1 Introduction

Recent progress in the area of nanophotonic device fabrication has rekindled an interest in building a nanophotonic integrated circuit. Materials such as high index contrast silicon-on-insulator [1], one-dimensional negative dielectric [2], photonic crystal [3, 4] and metal nanoparticle arrays utilising plasmon excitation [5–8] have been extensively investigated as possible ways to transmit light around or below diffraction-limit scales. In addition to the technologies listed, we have been working on nanophotonic devices based on colloidal quantum dots (QDs) because of their unique optoelectronic properties and flexible surface chemistry. Furthermore, since the principles of QD nanophotonic devices are fundamentally different from those of conventional devices, they provide a promising opportunity to reduce the size of photonic devices down to a few tens of nanometres. Fig. 1 shows the idea of an integrated circuit based on these QD nanophotonic devices. Previously, we have demonstrated fabrication and testing results for the nanoscale QD waveguide and QD photodetector [9, 10]. In this work, we explore the first step towards nanophotonic integration by developing a fabrication method to combine the QD waveguide with the QD photodetector.

2 Principle and device design

The QD waveguide consists of an array of densely packed QDs anchored to a substrate via self-assembly. The operation of the device, depicted in Fig. 2a, requires a pump laser of photon energy greater or equal to the separation of the second electron and hole states to be placed overhead to excite electron–hole pairs and enable gain. By aligning a signal laser with energy equivalent to the separation between the first electron and hole state to the input edge of the waveguide, photons generated by stimulated emission will cascade though the device, creating an amplified output that is moderated by the inter-dot coupling efficiency and the gain available in each dot. Finite-difference time-domain (FDTD) simulations of the electric field distribution in a QD cascade and cross-talk calculations based on the simulation results have been reported in support of the proposed device operation mechanism [11]. Moreover, sub-diffraction wave-guiding effect and reduced loss mechanism have been demonstrated for fabricated devices by performing transmission tests on both straight and right-angle 500 nm-wide QD waveguides [9].

The photodetector is fabricated by drop-casting QDs into a nano-gap in between a pair of Au electrodes, as shown in Fig. 2b. An applied electric field between the source and drain electrodes facilitates electron tunnelling and carrier extraction. The tunnelling current increases under photo excitation because of electron–hole pair generation in the colloidal QDs and subsequent charge-separation by the electric field. A responsivity of 0.029 A/W with ∼3 pA dark current for a fabricated device with 25 nm gap has been demonstrated [10]. By combining with a Keithley 6430 Sub-Femtoamp source meter and a Cascade Microtech M150 low-noise probe station, the photodetector shows measurable photocurrent under 5 pW of optical illumination. The responsivity of the photodetector can be increased by tuning the nano-gap size, and we have measured responsivity up to 0.15 A/W. The QD photodetector described here is not likely to outperform conventional PIN photodetectors in terms of responsivity owing to its low active volume. However, the main advantage of the nanoscale QD photodetector lies in its small size and spatial resolution, which allows integration with sub-diffraction optical waveguides that are closely spaced without compromising the integration density of the waveguides and the overall nanophotonic integrated circuits. The QD photodetector is fabricated upon silicon as shown in Section 3 and does not require epitaxial growth of the material, which makes integration with other nanophotonic waveguides such as nanowires, plasmonic materials, photonic crystals or high-index silicon-on-insulator devices readily achievable. In addition, the QD photodetector shows lower dark current compared with most of the conventional PIN

L. Huang and L.Y. Lin are with the Department of Physics, University of Washington, Seattle, WA 98195, USA

L.Y. Lin is with the Department of Electrical Engineering, University of Washington, Seattle, WA 98195, USA

M.C. Hegg and C.-J. Wang are with the Department of Electrical Engineering, University of Washington, Seattle, WA 98195, USA
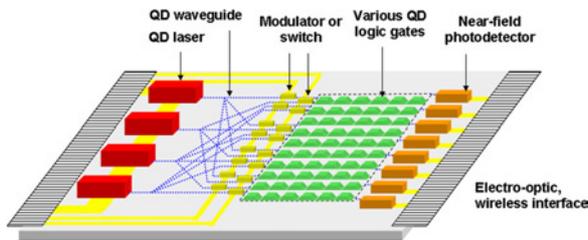
E-mail: lylin@u.washington.edu
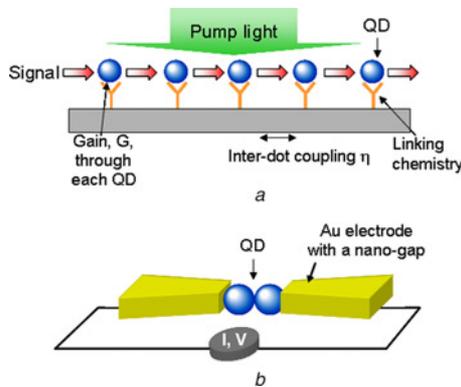
Fig. 1 *QD nanophotonic integrated circuit*

Fig. 2 *Schematic drawings of QD nanophotonic devices*
a QD waveguide
b QD photodetector

photodetectors, which normally have dark currents around 1 nA. There has been research on using single QDs as single-photon detectors by utilising a single-electron transistor [12] or by embedding an epitaxially grown QD layer in a field-effect transistor structure [13]. The former was demonstrated at very low temperatures (~ 70 mK) and the latter demonstrated photon counting over a dark-current floor of 80 pA. Ultra-sensitive solution-cast QD photodetectors with QDs embedded in a 5 μm × 3 mm area photoconductor structure has also been demonstrated [14]. The detector achieved a high responsivity of 10^3 A/W because of photoconductive gain, with dark current ranging from a few to hundreds of nanoAmperes.

Fig. 3 depicts the integrated device architecture. In this design, the optical signal at the receiving edge of the QD waveguide is guided to the output edge, where a QD
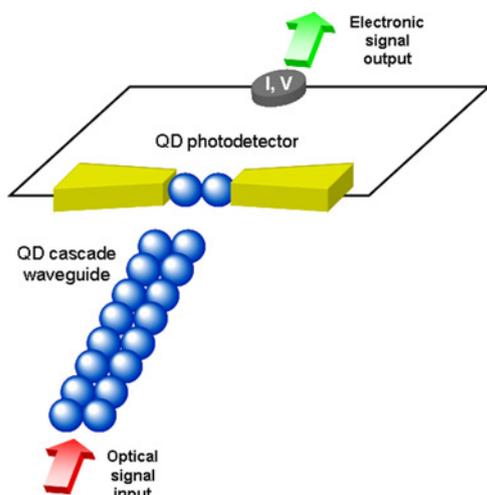

Fig. 3 *Schematic drawing of the QD nanophotonic waveguide and photodetector integrated device*

photodetector is positioned to receive the output signal. In other words, the optical signal is routed as desired and transformed to an electric signal, which can be further processed by on-chip electronic integrated circuits.

3 Fabrication

The fabrication of the integrated device is achieved by multiple alignment-assisted electron beam lithography (EBL) patterning of QD photodetector electrodes and QD waveguide, nano-gap formation in the electrode and self-assembled QD deposition. Among these steps, nano-gap formation is particularly critical to the device performance as QD photodetector testing has shown that nano-gaps ranging from 1 to 25 nm width yield different performance on signal-to-dark current ratio and responsivity. In the integrated device, the nano-gap formation is accomplished through both electromigration-induced break-junction technique and EBL nano-gap patterning. Both procedures are described below, and a comparison between the two methods is made in Section 4.

The first process, employing the electromigration-induced break-junction technique to create nano-gaps, is shown in Fig. 4 [15]. It begins with spin-coating polymethylmethacrylate (PMMA) on a Si/SiO₂ wafer and using EBL to define continuous electrode patterns with line widths of 50 nm. The exposed SiO₂ is then silanised with a monolayer of 3-mercaptopropyltrimethoxysilane (MPTMS). To perform silanisation, the wafer is exposed briefly to oxygen plasma to increase the number of –OH groups on the exposed SiO₂, and then to the MPTMS gaseous molecules inside a vacuum dessicator for 2 h. The –OH groups act as an anchor for vapour-phase self-assembly of MPTMS. The sample is then immediately transferred into a thermal evaporator for deposition of a 300-Å Au layer, followed by lift-off of PMMA to form the Au electrodes (Fig. 4*a*). The MPTMS monolayer acts as an insulating adhesion layer for the Au film. It is found that the addition of the MPTMS layer reduces direct tunnelling between the Au electrodes after the electromigration-induced break-junction process is performed without QD attachment, compared with other metal adhesion layers such as Cr. Next, following the procedure described in [16], a linearly increasing voltage is ramped across the Au electrode in steps of 0.1 mV at a rate of 0.1 mV/s until a 90% deviation from the original conductance is observed, because of the formation of a nano-gap. This process is known as the electro-induced break-junction technique [10, 16, 17]. After characterising the size and position of the nano-gaps using a scanning electron microscope (SEM), a second EBL is performed to define the waveguide
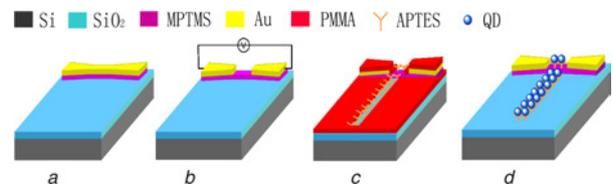

Fig. 4 *Fabrication process for making a nanophotonic waveguide and photodetector integrated device*

a Photodetector electrode patterned by EBL, 3′MPTMS deposition, Au evaporation and liftoff
b Nano-gap created by electromigration-induced break-junction technique
c Waveguide pattern aligned to the nano-gap is defined by a second EBL patterning
d Monolayer of QD deposition achieved through self assembly process with 3′APTES

pattern, which is aligned to the nano-gap in the electrode (Fig. 4c). The sample is then oxygen-plasma treated again to create −OH groups on the exposed SiO_2 surface and 3′aminopropyltriethoxylsilane (APTES) is deposited by immersion in solution to create a surface expressing amines for further chemical reaction [18]. A droplet of carboxylated QDs suspended in 1× phosphate buffer solution (PBS) mixed with 1-ethyl-3-(3-dimethylaminopropyl)−carbodiimide, an amine−carboxyl coupling reagent, is applied to the sample as the second layer. After waiting for a minimum of 1 h during which the QDs bind to the sample, excess material is rinsed off with 1× PBS buffer, and the PMMA is also removed with dichloromethane to reveal the waveguides (Fig. 4d) [9].

A modified integration process differs from the previous one in the formation of nano-gaps. Instead of the electromigration-induced break-junction technique, EBL patterning is used to create nano-gaps, which circumvents the serial process to create openings in the electrodes one-by-one. However, the switch in the method comes at the cost of achieving narrower gaps. Because of the proximity effect in EBL, which is more prominent when the size of designed patterns becomes close to that of the electron beam, the widths of the resultant nano-gaps are smaller than that of the original designed ones, depending on the originally designed nano-gap widths and EBL-writing parameters. To find the corresponding relationship between the width of a designed gap and that of the resultant gap, test EBL writings at different electron beam currents and dosages are performed. EBL writing can then be performed using the parameters that correspond to the optimal gap size indicated by the dose tests.

4   Results and discussion

We have fabricated nano-gaps ranging from 1 to 25 nm using the electromigration-induced break-junction technique described above. An example of the nano-gap is shown in Fig. 5, with a size of ∼3 nm. Previous researchers have demonstrated that the formation of nanometre gaps can be attributed to thermomigration [19] or electromigration [17] mechanisms, with a major difference in the dependence of threshold current density on sample temperature [19]. The electromigration mechanism can in general achieve smaller gaps than the thermomigration mechanism. According to the size of nano-gaps created by the procedure described in Section 3, we think the process is likely because of electromigration, although in general it is not easy to distinguish between both mechanisms.

Fig. 6 shows atomic force microscope (AFM) and SEM images, centred on the waveguide−photodetector junction region, of an integrated device in
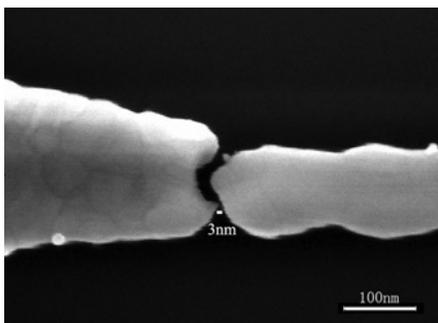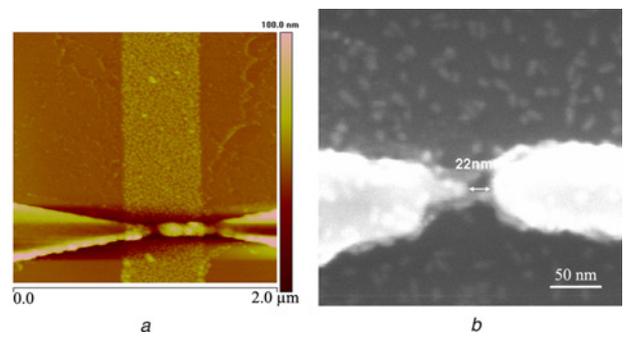

Fig. 6 *Micrographs of the integrated device employing electromigration-induced break-junction technique taken with*

a AFM
b SEM

which the electromigration-induced break-junction technique is employed as the nano-gap formation method. The AFM image demonstrates uniform distribution of QDs inside the ∼500 nm-width waveguide (Fig. 6a). The high-resolution SEM image further confirms the attachment of QDs inside the 22 nm gap between the photodetector electrodes. To optimise QD photodetector performance, nano-gaps in integrated devices are intentionally made with a larger size, as compared with typical gaps formed by electromigration. However, since both are created by the same procedure as that of the smaller gap shown in Fig. 5, we believe they are caused by the same mechanism.

Another integrated device by EBL nano-gap patterning and dual alignment procedure is shown in Fig. 7. The pre- and post-QD deposition images are shown in Figs. 7a and b, respectively. The adhesion layers employed for the devices in Figs. 6 and 7 are MPTMS and Cr, respectively. It is found that a gap size of 10−30 nm can be consistently achieved by writing at 30 kV, 15.0 pA current and a dose of 0.5−0.6 nC/cm with the EBL apparatus in use (FEI Sirion SEM). As can be seen from the SEM images, the EBL-patterned nano-gaps exhibit more abrupt edges and a cleaner break than those by electromigration-induced break-junction technique. For this particular integrated device, EBL nano-gap patterning also simplifies the process because it creates both the electrodes and nano-gaps in one EBL writing, whereas the electro-migration-induced break-junction process requires an additional step of breaking the junctions in series. Furthermore, EBL patterning provides more consistent control over the nano-gap size through lithography than the electromigration-induced break-junction technique, especially in the range of 10−30 nm. In addition, since there is no concern of metal residual interlink in the adhesion layer resulting from breaking the nano-electrode, the switch to EBL nano-gap
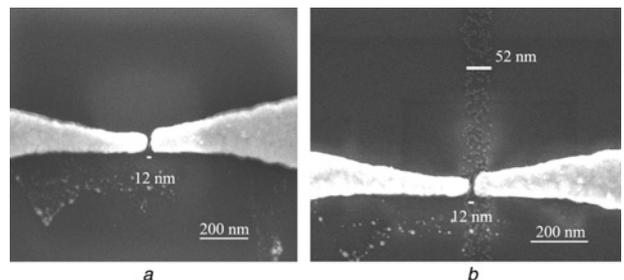

Fig. 5 *Typical nano-gap fabricated by electromigration-induced break-junction technique*

Fig. 7 *SEM micrographs of the integrated device by EBL nanogap patterning*

a Before integration of the waveguide and QD deposition
b After integration of the waveguide and QD deposition

patterning also makes it feasible to use Cr in place of MPTMS as the adhesion layer, which further shortens processing time.

Since multiple EBL writings are required to pattern different functional components in the integrated device, one of the chief challenges in fabrication is the issue of alignment accuracy. To achieve accurate alignment at the nanometre scale despite the common SEM sample moving stage error of ~ 5 μm, we adjust the position of the waveguide according to the position of nano-gaps and employ a coarse and fine two-step alignment procedure. The coarse alignment, comprising four 10 μm windows at pixel sizes of 100 nm each with an L-shape alignment mark inside, allows us to tolerate the stage error in the microscale and quickly find and roughly align the area of interest. Subsequently, we perform fine alignment using four 3 μm windows at pixel sizes of 10 nm with square alignment marks, which enables precise centring of the waveguide pattern with respect to the nano-gap, with an error of <20 nm. The twofold alignment allows us to decrease the width of waveguide down to ~ 50 nm while maintaining its position within the nano-gap, as shown in Fig. 7b.

In this first demonstration of QD waveguide and photodetector integrated device, we have used the same QDs for the waveguide and the photodetector. To optimise the performance of the integrated device, nanocrystals of different sizes can be chosen so that the emission peak of the waveguide QDs overlaps the absorption peak of the photodetector QDs. Deposition of multiple QD types can be achieved by introducing an additional EBL patterning to pattern the waveguide and nano-gap area separately.

5 Conclusions

We have demonstrated the fabrication of a QD waveguide and photodetector integrated device by alignment-assisted EBL patterning and QD self-assembly deposition. We have investigated two methods to create nano-gaps in the photodetector electrodes: electromigration-induced break-junction technique and EBL nano-gap patterning. Overall, EBL nano-gap patterning is preferable to the electromigration-induced break-junction technique for our integrated device in terms of resulting nano-gap quality, fabrication simplicity and consistency. Systematic characterisation of the position of nano-gaps combined with a coarse and fine two-step alignment procedure allows us to achieve an alignment error of <20 nm, which is essential for nano-scale photonic integration. The demonstrated result also shows that nanophotonic devices consisting of self-assembled colloidal QDs are attractive for achieving nanophotonic integrated circuits.

6 Acknowledgment

7 References

1 Barrios, C.A., Almeida, V.R., Panepucci, R., and Lipson, M.: 'Electrooptic modulation of silicon-on-insulator submicrometer-size waveguide devices', *J. Lightwave Technol.*, 2003, **21**, (10), pp. 2332–2339

2 Takahara, J., Yamagishi, S., Taki, H., Morimoto, A., and Kobayashi, T.: 'Guiding of a one-dimensional optical beam with nanometer diameter', *Opt. Lett.*, 1997, **22**, (7), pp. 475–477

3 Bogaerts, W., Baets, R., Dumon, P., Wiaux, V., Beckx, S., Taillaert, D., Luyssaert, B., Campenhout, J.V., Bienstman, P., and Thourhout, D.V.: 'Nanophotonic waveguides in silicon-on-insulator fabricated with CMOS technology', *J. Lightwave Technol.*, 2005, **23**, (1), pp. 401–412

4 Johnson, S.G., Villeneuve, P.R., Fan, S., and Joannopoulos, J.D.: 'Linear waveguides in photonic-crystal slabs', *Phys. Rev. B.*, 2000, **62**, (12), pp. 8212–8222

5 Brongersma, M.L., Hartman, J.W., and Atwater, H.A.: 'Electromagnetic energy transfer and switching in nanoparticle chain arrays below the diffraction limit', *Phys. Rev. B*, 2000, **62**, (24), pp. 16356–16359

6 Maier, S.A., Barclay, P.E., Johnson, T.J., Friedman, M.D., and Painter, O.: 'Low-loss fiber accessible plasmon waveguide for planar energy guiding and sensing', *Appl. Phys. Lett.*, 2004, **84**, (20), pp. 3990–3992

7 Maier, S.A., Kik, P.G., Atwater, H.A., Meltzer, S., Harel, E., Koel, B.E., and Requicha, A.A.G.: 'Local detection of electromagnetic energy transport below the diffraction limit in metal nanoparticle plasmon waveguides', *Nature Mater.*, 2003, **2**, (4), pp. 229–232

8 Yatsui, T., Nomura, W., and Ohtsu, M.: 'Self-assembly of size- and position-controlled ultralong nanodot chains using near-field optical desorption', *Nano Lett.*, 2005, **5**, (12), pp. 2548–2551

9 Wang, C.-J., Huang, L., Parviz, B.A., and Lin, L.Y.: 'Sub-diffraction photon guidance by quantum dot cascades', *Nano Lett.*, 2006, **6**, (11), pp. 2549–2553

10 Hegg, M.C., and Lin, L.Y.: 'Nano-scale nanocrystal quantum dot photodetectors' (CLEO/QELS, Baltimore, MD, 6–11 May 2007)

11 Huang, L., Wang, C.-J., and Lin, L.Y.: 'Comparison of cross-talk effects between colloidal quantum dot and conventional waveguides', *Opt. Lett.*, 2007, **32**, (3), pp. 235–237

12 Astafiev, O., and Komiyama, S.: 'Single-photon detection with quantum dots in the far-infrared/submillimeter-wave range' in Bird, J.P. (Ed.) 'Electron transport in quantum dots', (Kluwer Academic Press, Boston, 2003, 1st edn.), pp. 363–396

13 Gansen, E.L., Rowe, M.A., Greene, M.B., Rosenberg, D., Harvey, T.E., Su, M.Y., Hadfield, R.H., Nam, S.W., and Mirin, R.P.: 'Photon-number-discriminating detection using a quantum-dot, optically gated, field-effect transistor', *Nature Photonics*, 2007, **1**, (10), pp. 585–588

14 Konstantatos, G., Howard, I., Fischer, A., Hoogland, S., Clifford, J., Klem, E., Levina, L., and Sargent, E.H.: 'Ultrasensitive solution-case quantum dot photodetectors', *Nature*, 2006, **442**, (7), pp. 180–183

15 Huang, L., Hegg, M.C., Wang, C.-J., and Lin, L.Y.: 'Fabrication of a nanophotonic waveguide and photodetector integrated device'. OSA Nanophotonics Topical Conference, Hangzhou, China, 18–21 June, 2007

16 Mahapatro, A.K., Ghosh, S., and Janes, D.B.: 'Nanometer scale electrode separation (nanogap) using electromigration at room temperature', *IEEE Trans. Nanotechnol.*, 2006, **5**, (3), pp. 232–236

17 Park, H., Lim, A.K.L., and Alivisatos, A.P.: 'Fabrication of metallic electrodes with nanometer separation by electromigration', *Appl. Phys. Lett.*, 1999, **75**, (2), pp. 301–303

18 Demers, L.M., Ginger, D.S., Park, S.J., Li, Z., Chung, S.W., and Mirkin, C.A.: 'Direct patterning of modified oligonucleotides on metals and insulators by dip-pen nanolithography', *Science*, 2002, **296**, (5574), pp. 1836–1838

19 Ramachandran, G.K., Edelstein, M.D., Blackburn, D.L., Suehle, J.S., Vogel, E.M., and Richter, C.A.: 'Nanometre gaps in gold wires are formed by thermal migration', *Nanotechnology*, 2005, **16**, (8), pp. 1294–1299